Apigenin Attenuates Hippocampal Microglial Activation and Restores Cognitive Function in Methotrexate-Treated Rats: Targeting the miR-15a/ROCK-1/ERK1/2 Pathway

Mohamed Taha[1] · Omar Mohsen Eldemerdash[2] · Ismail Mohamed Elshaffei[2] · Einas Mohamed Yousef[3] · Ayman S. Soliman[4] · Mahmoud Ahmed Senousy[1,5]

© The Author(s) 2023

Abstract

Microglial activation underpins the methotrexate (MTX)-induced neurotoxicity; however, the precise mechanism remains unclear. This study appraised the potential impact of apigenin (Api), a neuroprotective flavonoid, in MTX-induced neuro-toxicity in rats in terms of microglial activation through targeting the miR-15a/Rho-associated protein kinase-1 (ROCK-1)/extracellular signal-regulated kinase 1/2 (ERK1/2) pathway. Male Sprague Dawley rats were randomly divided into 4 groups: Normal control (saline i.p. daily and i.v. on days 8 and 15); Api control (20 mg/kg, p.o.) daily for 30 days; MTX-alone (75 mg/kg, i.v.) on days 8 and 15, then four i.p. injections of leucovorin (LCV): 6 mg/kg after 18 h, then three doses (3 mg/kg) every 8 h post-MTX; and Api co-treated (20 mg/kg/day, p.o.) throughout the model for 30 days, with administration of MTX and LCV as in group 3. MTX administration elevated hippocampal ionized calcium-binding adaptor protein-1 (Iba-1) immunostaining, indicating microglial activation. This was accompanied by neuroinflammation, oxidative stress, and enhanced apoptosis manifested by elevated hippocampal interleukin-1β, malondialdehyde, and caspase-3, and decreased reduced glutathione levels. Concurrently, abated miR-15a expression, overexpression of its target ROCK-1, diminished downstream ERK1/2 and cAMP response element-binding protein (CREB) phosphorylation, and decreased hippocampal brain-derived neurotrophic factor (BDNF) levels were observed. Api mitigated the MTX-induced neurotoxicity by reversing the biochemical, histopathological, and behavioral derangements tested by novel object recognition and Morris water maze tests. Conclusively, Api lessens MTX-induced neuroinflammation, oxidative stress, and apoptosis and boosts cognitive function through inhibiting microglial activation via modulating the miR-15a/ROCK-1/ERK1/2/CREB/BDNF pathway.

Abbreviations
ALL	Acute lymphoblastic leukemia
AD	Alzheimer's disease
Api	Apigenin
BDNF	Brain-derived neurotrophic factor
CA	Cornu ammonis
CMC	Carboxymethyl cellulose
CREB	cAMP response element-binding protein

✉ Mohamed Taha
mohamed.taha@pharma.cu.edu.eg

Omar Mohsen Eldemerdash
omar.eldemerdash@miuegypt.edu.eg

Ismail Mohamed Elshaffei
ismail.shaffei@miuegypt.edu.eg

Einas Mohamed Yousef
enasesawy@gmail.com

Ayman S. Soliman
ayman.soliman@med.bsu.edu.eg

Mahmoud Ahmed Senousy
mohmoud.ali@pharma.cu.edu.eg; msenowsy@ecu.edu.eg

[1] Department of Biochemistry, Faculty of Pharmacy, Cairo University, Kasr El Ainy st., Cairo 11562, Egypt

[2] Department of Biochemistry, Faculty of Pharmacy, Misr International University (MIU), KM 28 Cairo, Ismailia Road, Cairo 44971, Egypt

[3] Department of Histology and Cell Biology, Faculty of Medicine, Menoufia University, Shibin El Kom, Egypt

[4] Medical Physiology Department, Faculty of Medicine, Beni-Suef University, Beni-Suef, Egypt

[5] Department of Biochemistry, Faculty of Pharmacy and Drug Technology, Egyptian Chinese University, Cairo 11786, Egypt

DG   Dentate gyrus
DI   Discrimination index
ELISA   Enzyme-linked immunosorbent assay
ERK1/2   Extracellular signal-regulated kinase 1/2
GSH   Reduced glutathione
Iba-1   Ionized calcium-binding adaptor protein-1
IHC   Immunohistochemistry
IL-1β   Interleukin-1β
LCV   Leucovorin
MDA   Malondialdehyde
miR-15a   MicroRNA-15a
MTX   Methotrexate
MWM   Morris water maze
NOR   Novel object recognition
PI   Preference index
ROCK-1   Rho-associated protein kinase-1
RT-qPCR   Reverse transcriptase-quantitative polymerase chain reaction
SD   Standard deviation

Introduction

Methotrexate (MTX) is one of the most routinely employed chemotherapeutic agents in acute lymphoblastic leukemia (ALL) and other cancers; however, its use has been linked to an increased incidence of neurotoxicity in about 9–53% of patients [1, 2]. This is evident as cognitive impairment, memory problems, and motor dysfunction which appear in 30–60% of pediatric cancer survivors who have undergone chemotherapy [2, 3]. The severity of MTX-induced neurotoxicity is multifactorial, with many predisposing factors influencing its severity, including age, dose, route of administration, and exposure to radiation [3]. Although several theories have been proposed to contemplate the neurotoxic actions of MTX, the exact mechanism is still unknown.

Microglial activation, neuroinflammation, and activation of apoptosis are among the mechanisms expected to be involved in MTX-induced neurotoxicity, ultimately culminating in loss of spatial working memory and cognitive impairments [4]. Indeed, Wen et al. [5] reported that 50% of MTX-treated rats showed a substantial decrease in hippocampal neurogenesis, cell proliferation as well as increased microglial activation and apoptosis compared to controls [5]. Peculiarly, MTX was reported to activate the microglia, prompting escalated inflammatory response [6]. The microglia are neuronal macrophages, which release chemokines and cytokines, activate apoptosis, inhibit cell proliferation, and maturation [7]. Persistent activation of the inflammatory microglia can cause neurotoxicity by dysregulation of astrocytes and oligodendrocytes, decreasing neuronal myelination, survival, and neurogenesis, and increasing neuroinflammation, finally precipitating cognitive impairment and memory deficits [6, 8]. Recently, MTX was shown to induce chronic microglial activation [6, 9]. However, the exact molecular pathway is still unclear.

Recent studies demonstrate the crucial role of Rho-associated protein kinase-1 (ROCK-1) in various neurodegenerative diseases [10, 11]. ROCK-1 plays a critical role in microglial inflammatory cytokine synthesis and release via controlling microglial activation [12]. Inhibition of ROCK-1 activity was reported to affect the microglial phenotype, which might contribute to the neuroprotective effects noted following ROCK-1 inhibition in various models [13–15]. Furthermore, ROCK-1 induction increases neuroinflammation not only via microglial activation but also by its down-regulatory effect on extracellular signal-regulated kinase 1/2 (ERK1/2) and the downstream mediators cAMP response element-binding protein (CREB)/brain-derived neurotrophic factor (BDNF) [16]. These data emphasize the possible role of the ROCK-1/ERK1/2 pathway in microglial activation, but whether this extends to the MTX-induced neuroinflammation has not been previously tackled.

Recently, microRNAs (miRNAs) have been interconnected with memory regulation and neurogenesis. Among various miRNAs, miR-15a was demonstrated to be downregulated in Alzheimer's disease (AD) brains; its overexpression has been proven to improve spatial memory and cognitive performance in AD mice models [17]. A recent study has shown that miR-15a targets and represses the ROCK-1 gene in hippocampus neurons, and that its increased expression boosted cell survival while decreasing apoptosis [18]. However, the effect of MTX on miR-15a and its downstream ROCK-1 as well as their impact on microglial activation is poorly elucidated.

Apigenin (Api) is a flavonoid that occurs naturally in a range of fruits and vegetables, including chamomile flowers, garlic, parsley, guava, onion, tea, and citrus fruits [19]. Among the many recognized biological effects of Api are its antioxidant and anti-inflammatory properties as well as its ability to fight cancer and other serious diseases [20]. The neuroprotective effect of Api was recently identified in a rat model of pentylenetetrazol-induced cognitive impairment [19] as well as in vitro models of neuroinflammation associated with AD [21]. However, the full neuroprotective and restorative mechanisms of Api are still to be investigated.

With this scenario, we hypothesized that Api has the premise as a beneficial candidate for co-treatment with MTX to mitigate its neurotoxic effects and behavioral and memory derangements. Thereby, this study was designated to investigate the potential involvement of the miR-15a/ROCK-1/ERK1/2 pathway in MTX-induced neurotoxicity in rats from the perspective of microglial activation. Specifically, the neuroprotective effect of Api was examined in terms of its impact on miR-15a/ROCK-1/ERK1/2/CREB/BDNF pathway, microglial activation, neuroinflammation, oxidative stress, and apoptosis. Microglial activation was examined using the immunofluorescence staining of ionized calcium-binding adaptor protein-1 (Iba-1).

Materials and Methods

Experimental Animals

Sixty male Sprague Dawley rats, weighing 150–200 g and aged 4–5 weeks, were obtained. The animals were kept in propylene cages (5 per cage) in a controlled environment at Misr International University's animal house, with a consistent temperature (25 °C ± 2 °C), humidity (60 ± 10%), and a 12/12-h light/dark cycle as well as unrestricted access to water and pellet diet.

The Research Ethics Committee for Experimental and Clinical Studies, Faculty of Pharmacy, Cairo University, Cairo, Egypt, authorized all animal procedures and experimental protocols (Permit Number: BC2944). The animals were housed according to the US National Institutes of Health publication Guide for Care and Use of Laboratory Animals (No. 85–23, revised 2011). All attempts were made to reduce the number of animals used and minimize animal suffering.

Drugs and Chemicals

MTX was procured from Mylan S.A.S., France as 50 mg/vial ready for intravenous (i.v.) administration. Api (50 mg/capsule) was purchased from Swanson, USA; each capsule was dissolved into 10 ml of 0.5% carboxymethyl cellulose (CMC) immediately before oral administration. Leucovorin (LCV) (Calcifolinon®, 50 mg/vial) was supplied from GPI, Egypt. CMC sodium salt was purchased from TopChem, Egypt.

Experimental Design

During the design phase of the experiment, we conducted a pilot study in which we found that the administration of four i.p. doses of LCV following MTX administration is vital to maintain the rats alive by lessening the MTX-induced fatal diarrhea and weight loss. The significant mortality rate in the pilot study led us to start the study model with 15 rats/group to ensure sufficient samples at the end of the experiment.

Rats were randomly divided into four groups of 15 rats each. The group size was calculated using power analysis (power = 0.9, α = 0.05). The rats had been acclimated to the new environment for 7 days. The experimental design is displayed in Fig. 1 as follows:

Group 1 (Normal control): rats received saline intraperitoneally daily for 30 days and intravenously on the 8th and 15th days of the model.
Group 2 (Api control): rats received a daily dose of Api (20 mg/kg, p.o.) dissolved in 0.5% CMC for 30 days [19].
Group 3 (MTX only): rats received MTX (75 mg/kg, i.v.) on the 8th and 15th days of the model [22], afterwards they received four i.p. injections of LCV: the first dose was 6 mg/kg after 18 h, and the following three doses were 3 mg/kg after 26, 42, and 50 h of MTX administration [22–24].
Group 4 (Api co-treated): Api (20 mg/kg/day, p.o.) was administered daily to rats throughout the study for 30 days, with administration of MTX (75 mg/kg, i.v.) on days 8 and 15, followed by LCV injections as in group 3.

All doses were selected based on previously published data. All models studying MTX-induced neurotoxicity were 30 days long in which MTX (75 mg/kg, i.v.) is administrated on both the 8th and 15th days of the model [22, 24]. Api was administered in 20 mg/kg, p.o. based on a previous trial which supported the use of 20 mg/kg over the use of 10 mg/kg in attenuating cognitive impairment and CREB/BDNF upregulation in kindled mice [19]. Furthermore, Api was used in the same dose as hepatoprotective and neuroprotective flavonoid in bile duct ligation [25] and in nephropathy [26]. LCV doses were chosen based on previous studies [22–24] and our pilot study.

Fig. 1 Experimental design
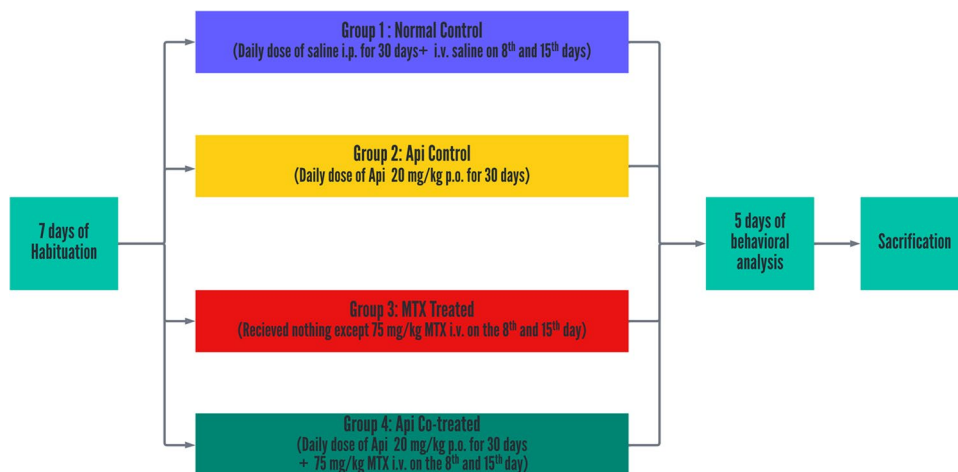
Assessments of the rats' memory and cognitive functions were carried out after 30 days for all groups (10 rats per group). Twenty-four hours following the behavioral testing, sacrification was performed by cervical dislocation after being anesthetized with 3% isoflurane inhalation. Right away, brains were dissected and quickly rinsed in ice-cold saline. Four whole brains from each group were fixed in 10% neutral buffered formalin, and then sent to the pathology lab for histopathological and immunohistochemical examination. The hippocampi of the remaining six brains were dissected from each side of the brain and frozen at − 80 °C until the biochemical parameters were tested. All assessments were conducted by blinded investigators.

Behavioral Tests

Novel object recognition (NOR) and Morris water maze (MWM) were selected due to their effectiveness in assessing memory and cognitive function, their availability in the animal house, and the availability of ANY-maze software for automatic analysis. NOR is a frequently utilized behavioral examination for spatial memory that investigates the short- and long-term spatial memory associated with the hippocampus [27, 28]. Furthermore, MWM is utilized to identify spatial learning and memory in hippocampal-affected animals [28].

NOR Test

At the end of the model, NOR was carried out in order to evaluate the rats' capacity to recall the previously studied object and identify the new one. Each animal was trained for 5 min in an empty open field arena (1 m × 1 m × 0.5 m) the day before the test. On the day of the examination, every rat participated in two trials: a familiarization trial and a choice trial. Both trials were monitored, recorded, and analyzed with the help of ANY-maze software. After each test, the arena and the objects in it were disinfected with ethanol at a concentration of 20% to eradicate any trace of a scent.

During the familiarization phase of the experiment, each rat was exposed to two of the same objects. After allowing each rat to investigate the items for a period of 3 min, they were removed from the arena and placed in a separate cage for a period of 15 min. After this period of time had passed, one of the objects that were being used in the choice experiment was switched out for a brand-new object. During the choice trial, each rat was taken back to the arena and presented with one familiar object and one unfamiliar object. They were given 3 min to investigate the items before being taken out of the arena and returned to their regular cages. The amount of time spent investigating each object while the rat's head was pointed toward the thing from a distance of less than 2 cm away from the object was logged [23].

MWM Test

The MWM test was used to determine the rats' spatial learning ability. The rats began the training phase of the MWM 1 day after the model ended, with 12 training trials in which each rat received four training trials per day for three consecutive days before receiving a probe trial [29]. During the training phase, the platform was positioned in the pool's south-east (SE) quadrant. Each rat began a 1-min trial from one of four different starting locations, and each rat received four different trials from each starting position on a daily basis, as shown in Table 1. Each trial was limited to 1 min in duration, and if the rat did not reach the platform, it was directed to it for 15 s before being returned to its cage. The rats received 1 h of rest in between trials. On the fourth day, the rats had the probe test in which the platform was removed. The rats started from the NW position for 1 min. The quadrant time percentage, path efficiency, and escape latency were detected. ANY-maze software was used to record and analyze the trials and the probe trial.

miRNA Selection

We relied on a bioinformatics approach using the miRTargetLink 2.0 interactive tool (https://ccb-compute.cs.uni-saarland.de/mirtargetlink2/network/bf99b12a-cd13-453e-bcc1-aa4226ac943e) as well as on previously reported experimental validation to confirm the interaction of miR-15a and ROCK-1 [18]. We also employed the Human MicroRNA Disease Database (HMDD) (https://www.cuilab.cn/hmdd) to detect the association between the selected miRNA and neurological disorders. Indeed, the association of miR-15a with AD, epilepsy, and multiple sclerosis was recorded in the database.

Biochemical Assays

Homogenization of rat brain hippocampal tissue was processed as directed by the manufacturer using cold phosphate-buffered saline, and a 10% tissue homogenate was prepared.

Table 1 Morris water maze start positions

Day	Trial 1	Trial 2	Trial 3	Trial 4
Day 1	N	W	SW	NE
Day 2	SW	N	NE	W
Day 3	NE	SW	W	N
Day 4	Probe trial started at NW			

N, North; *W*, West; *SW*, South-west; *NE*, North-east; *NW*, North-west

Colorimetric Assay

Reduced glutathione (GSH) and malondialdehyde (MDA) concentrations were determined using colorimetric kits manufactured by Biodignostics®, Giza, Egypt (Cat. No. GR 25 11, MD 25 29). All assays were conducted in accordance with the manufacturer's specifications in a 10% hippocampal tissue homogenate.

Enzyme-Linked Immunosorbent Assay (ELISA)

For the analysis of total CREB (t-CREB), phosphorylated CREB (p-CREB), BDNF, interleukin (IL)-1β, and caspase-3, rat ELISA kits were used. The total CREB and p-CREB ELISA kits were purchased by FineTest®, China (Cat. No: ER0914) and AFG Bioscience®, USA (Cat. No: EK742597), respectively. BDNF and IL-1β ELISA kits (Cat. No: E-EL-R2084 for BDNF and Cat. No. E-EL-R0267 for IL-1β) were manufactured by Elabscience®, USA. The caspase-3 ELISA kit was obtained from Cusabio®, USA (Cat. No: CSB-E07264r). Following the manufacturer's instructions, all tests were carried out on a 10% hippocampal tissue homogenate using the Sandwich ELISA technique.

Data of ELISA and colorimetric assays are expressed per mg protein as measured using Bradford method.

Reverse Transcriptase-Quantitative Polymerase Chain Reaction (RT-qPCR)

Total RNA was deduced from lysates of rat brain hippocampal tissue using Direct-zol RNA Miniprep Plus (Cat. No. R2072, Zymo Research Crop, USA), according to the manufacturer's protocol. A Beckman dual spectrophotometer (USA) was used to determine the concentration and purity of the extracted RNA. The optical density of isolated RNA was determined at 260 nm and 280 nm to guarantee its purity. The entire RNA was reverse transcribed into complementary DNA (cDNA). For analyzing the expression levels of miR-15a and ROCK-1, we utilized Thermo Fisher Scientific's Superscript IV One-Step RT-PCR kit (Cat. No. 12594100, USA) for reverse transcription and real-time PCR in a single step using Step-One Applied Biosystem PCR apparatus, USA according to the manufacturer's protocol. The primers' sequences of the studied genes and the reference genes are mentioned in Table 2.

The results of RT-qPCR were translated into cycle threshold (Ct) values. The Ct values for the studied genes miR-15a and ROCK-1 were determined and corrected using the delta-delta Ct method normalizing to the housekeeping genes RNU6 and GAPDH, respectively. We determined the fold change of each gene by taking $2^{-\Delta\Delta Ct}$.

Table 2 Sequences of primers used in the study

Gene	Accession number	Primer sequence (5'-3')
miR-15a	XR_005648635.1	F: GCCGAGTAGCAGCACACATAA
		R: CAGTGCGTGTCGTGGAGT
RNU6	XR_006711274.1	F: GCTTCGGCAGCACATATA CTAAA
		R: CGCTTCACGAATTTGCGT GTCAT
ROCK-1	NR_171200.1	F: AATCTTCCAGTTGGTTCTGCCT
		R: CTCTATTTGGTACAGAAAGCC AACC
GAPDH	NM_001394060.2	F: CCTTCTCCATGGTGGTGAAGA
		R: CACCATCTTCCAGGAGCGAG

Western Blotting

Total and phosphorylated ERK1/2 (p-ERK1/2) levels in hippocampal tissues were measured using a western blot. The ReadyPrep® complete protein extraction kit from BIO-Rad Inc., USA (Cat. No. 163–2086) was used to extract protein. BIO Basic Inc., Canada's Bradford Protein Assay Kit (Cat. No. SK3041) was used to assess protein concentration in each sample. Each 20 µg protein sample was then loaded with 2 × Laemmli sample buffer containing 4% sodium dodecyl sulphate (SDS), 10% 2-mercaptoethanol, 20% glycerol, 0.004% bromophenol blue, and 0.125 M Tris HCl, and the pH was adjusted to 6.8. The mixture was heated at 95 °C for 5 min before polyacrylamide gel electrophoresis to denature the protein. Polyacrylamide gels were made with Bio-Rad Laboratories Inc. TGX Stain-Free™ FastCast™ Acrylamide Kit (SDS-PAGE) (Cat. No: 161–0181). The SDS-PAGE was made as directed. From bottom to top, the gel was built in a transfer sandwich (filter paper, PVDF membrane, gel, and filter paper). The sandwich was placed in 1 × transfer buffer (25 mM Tris, 190 mM glycine, and 20% methanol). Next, protein bands were transferred from the gel to the membrane at 25 V for 7 min using a Bio-Rad Trans-Blot Turbo. For 1 h, the membrane was occluded in Tris-buffered saline (TBS) blocking buffer components: 3% bovine serum albumin, 0.1% Tween 20, 20 mM Tris, 150 mM NaCl, pH 7.5. We used p-ERK1/2 and total ERK1/2 primary antibodies [diluted 1:500 in Tris-buffered saline and Tween (TBST)]. Each primary antibody was incubated overnight at 4 °C. The blot needed 3–5 TBST rinses over 5 min. The target protein was incubated in the horseradish peroxidase (HRP)-conjugated secondary antibody solution for 1 h at room temperature as previously described [30].

The chemiluminescent substrate (Clarity™ Western ECL substrate Bio-Rad Cat. No: 170–5060) was added to the blot in accordance with the manufacturer's instructions.

CCD camera-based imagers recorded the chemiluminescent signals. ChemiDoc MP imager band intensities were compared to β-actin (housekeeping protein) using image analysis tools.

Histopathology and Immunohistochemistry

After being cleaned and fixed in 10% neutral buffered formalin for 72 h, samples were washed with xylene, infiltrated, and then embedded in Paraplast tissue embedding media after being trimmed and treated with different grades of ethanol. Hippocampal regions in distinct samples were demonstrated using rotary microtome sections of 4-µm-thick sagittal brain.

The general morphological examination was performed using H&E staining. In Dentate gyrus (DG) and Cornu ammonis (CA3), Nissl staining with toluidine blue staining was used to identify damaged and intact neurons. The Handbook of Histopathological and Histochemical Techniques was followed for all fixation and staining procedures [31].

To perform immunohistochemistry, preparation of 5-µm-thick paraffin embedded tissue sections was carried out in line with the manufacturer's instructions. 0.3% H_2O_2 was applied to deparaffinized tissue sections for 20 min. Afterwards, anti-Iba-1 antibody was used to treat the brain samples overnight at 4 °C (ab108539-Abcam — 1:100). After washing with phosphate-buffered saline, tissue sections were incubated for 20 min with the HRP Envision kit (DAKO) secondary antibody. The sample was then washed and incubated for 15 min with diaminobenzidine. The sample was then dehydrated, cleaned in xylene, and covered for microscopic examination.

According to Abbas et al. [32], Iba-1 immuno-expression levels in immunohistochemically stained sections were determined by the image analyzer computer system; Image J software (Version 1.53 K, National Institute of Health, USA) using six non-overlapping fields from each sample [32]. Furthermore, the number of intact neurons in both DG and CA3 was assessed using the same software [33]. The Leica Application module for histological analysis and a full HD microscopic imaging system (Leica Microsystems GmbH, Germany) were used for all light microscopic exams and data acquisition.

Statistical Analysis

G*Power software was used to calculate the sample size per group using power analysis (power = 0.9, α = 0.05). The mean and standard deviation (SD) were utilized to mathematically express the data. The tests of Shapiro–Wilk and Kolmogorov–Smirnov were used to determine whether the variables in this study followed a normal distribution. One-way ANOVA with Tukey's post hoc test was performed to compare the results of the various groups, except for the training and probe escape latency where two-way ANOVA was used. The Dixon Q test was utilized to identify the outliers. Mead's "Resource Equation" was applied to evaluate whether the sample size is statistically sufficient. All statistical analyses were carried out with the help of the GraphPad Prism 9.0.0 statistical analysis program (121). The correlations between various parameters were analyzed using Pearson's correlation. For each test, a P value of less than 0.05 was used to show statistical significance.

Results

Api Restores Cognitive Function in MTX-Treated Rats

The discrimination index (DI) is the difference between the amount of time spent exploring a novel object and the amount of time spent exploring a familiar object, divided by the total amount of time spent exploring both novel and familiar objects [$DI = (T_N - T_F) / (T_N + T_F)$]. Noticeably, the Api-control group was similar to the normal control group in all measured parameters. The DI was significantly decreased by 1.36 folds in the MTX-induction group compared with that in the control group. However, Api co-treatment pre- and post-MTX administration meaningfully increased the DI by 2.12 folds compared with its level in the MTX-alone group (Fig. 2A).

The preference index (PI) was determined by dividing the time spent exploring the novel object by the total time spent investigating both novel and familiar objects, and then multiplying the result by 100. In the MTX group, the PI dropped by 82.9% in comparison with that in the normal control group. However, Api co-treatment significantly raised the PI by 4.4-fold (Fig. 2B).

In MWM, we observed that the quadrant time percentage (the proportion of time the rat spent in the target quadrant during the probe test) was 52% lower in the MTX group compared with that in the normal control group. On the other hand, the quadrant time increased by 1.63-fold in the Api co-treated group compared with that in the MTX group (Fig. 3A). The path traveled by the rats was tracked by the ANY-maze software and plotted in the track plots, which clearly indicate that the Api co-treated group spent more time in the quadrants than the MTX group (Fig. 3E–H). In addition, we observed the path efficiency, which is the ratio of the actual path length traveled by a rat to the optimum path it could have taken to reach the target quadrant. The MTX group demonstrated a roughly 60% decline in path accuracy relative to the control group; however, the Api co-treated rats demonstrated a 3.4-fold increase in path efficiency relative to the MTX group (Fig. 3B).

Fig. 2 Effects of MTX and Api co-treatment on cognitive function (novel object recognition test). Data are expressed as mean ± SD, $n = 10$. (**a**) significant difference from control, (**b**) significant difference from MTX. Significance level was set at $P < 0.05$. One-way ANOVA test and Tukey's post hoc test were used in the statistical analysis
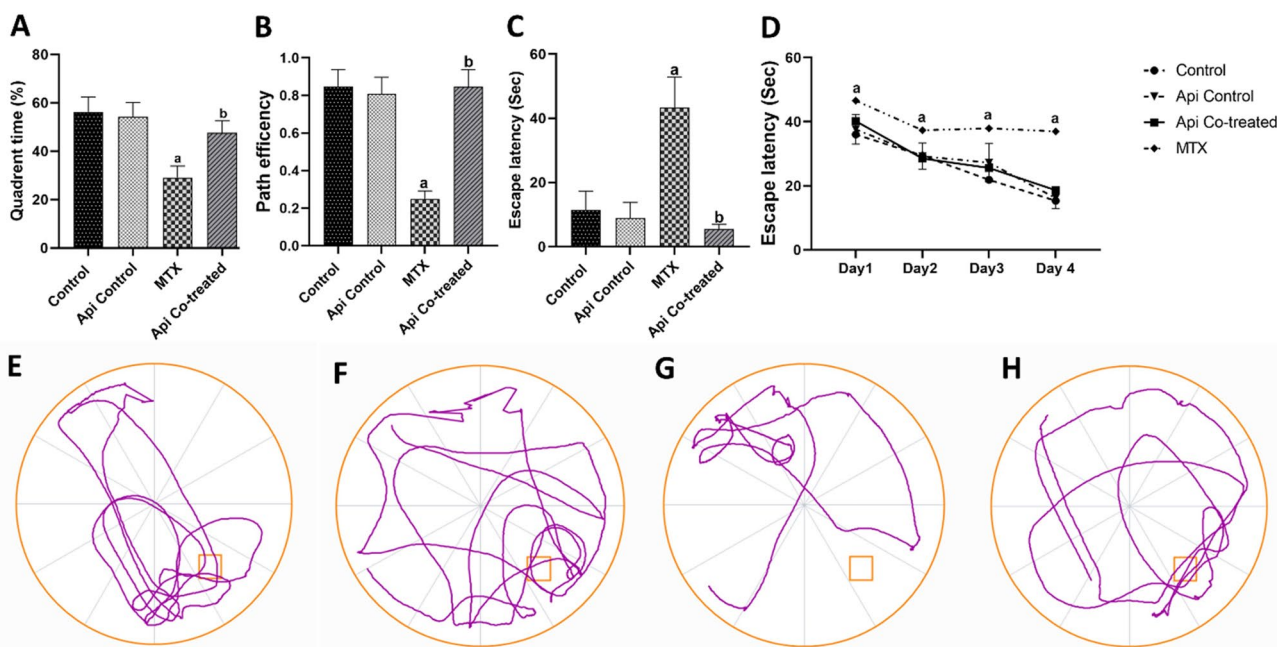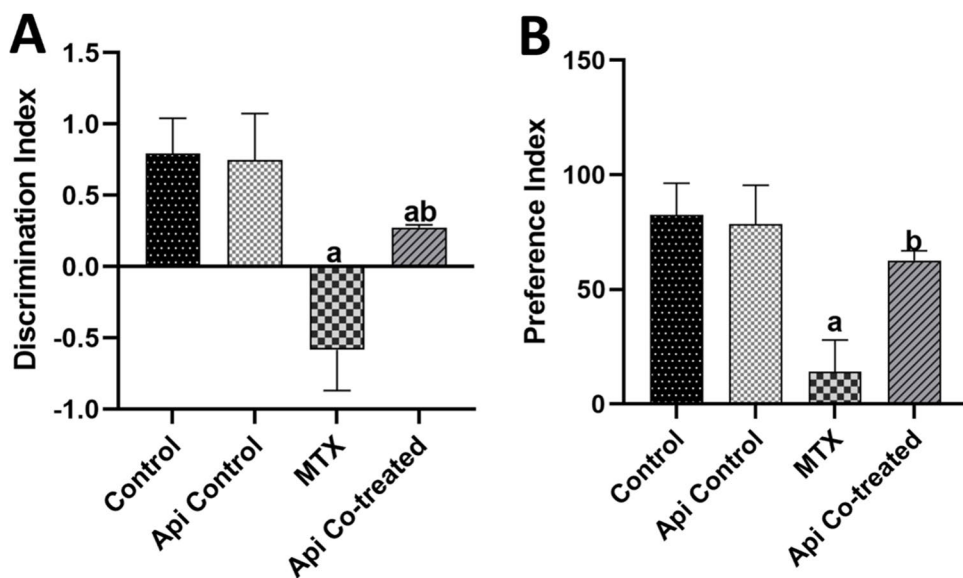

Fig. 3 Effects of MTX and Api co-treatment on cognitive function (Morris water maze test). **A** quadrant time, **B** path efficiency, **C** escape latency for probe test, **D** escape latency for training days (days 1–3) and probe test (day 4), **E** track plot for normal control, **F** track plot for Api control, **G** track plot for MTX, and **H** track plot for Api co-treated. Data are expressed as mean ± SD, $n = 10$. (a) significant difference from control, (b) significant difference from MTX. Significance level was set at $P < 0.05$. One-way ANOVA test and Tukey's post hoc test were used in the statistical analysis, except fot the training and probe escape latency where two-way ANOVA was used

Furthermore, the escape latency was measured to appraise the learning ability of the rats. Rats in the MTX group took 3.79 folds longer time to reach the platform area than normal rats. Api co-treatment throughout the study significantly reverted the learning ability of rats back to the control levels as it showed a noticeable decrease in the escape latency time by 87.24% of that in the MTX group (Fig. 3C). Examining the escape latency during the training trials (days 1–3) and the probe test (day 4) to examine the learning pattern of rats revealed that the MTX group had lower learning ability and the escape latency progress over days than the control and Api co-treated groups (Fig. 3D).

Api Modulates miR-15a/ROCK-1 in the Hippocampus of MTX-Treated Rats

MTX administration abated the expression of miR-15a in the hippocampus reaching 12.6% of the normal control values. This was accompanied by an increase in the levels of its downstream target ROCK-1 by 3.51 folds in comparison with levels in the control rats (Fig. 4A,B). These results highlighted the neurotoxic effect of MTX on the molecular level.

The Api co-treated group exhibited a significant escalation in the expression levels of miR-15a by 4.63 folds compared with those in the MTX-alone group (Fig. 4A). This increase obviously led to a decline in the ROCK-1 transcription factor level by 54.46% (Fig. 4B), suggesting Api as a possible co-treatment to restore the neuroprotective miR-15a levels.

Api Mitigates the MTX Effect on the Hippocampal ERK1/2/CREB/BDNF Pathway

In the context of ROCK-1 elevation in the MTX group, the expression of t-ERK1/2 was not affected; however, its activation was reduced. This was marked by the observed downregulation of p-ERK1/2 levels by 88.47% as well as an 8.71-fold reduction in p-ERK/t-ERK ratio in the MTX-treated rats compared with levels in the normal control rats (Fig. 5A–D). Subsequently, p-CREB, t-CREB levels, and p-CREB/t-CREB ratio were recorded to decline in the hippocampus by 48.66%, 28.1%, and 28.64%, respectively,

in the MTX group compared with the normal control values (Fig. 6A–C). Moreover, the hippocampal BDNF levels were found to be 25.96% lower in the MTX group than that in the normal control rats (Fig. 6D).

Herein, the neuroprotective effect of Api was set clear by its effect on the ERK1/2/CREB/BDNF pathway. Downstream of ROCK-1, t-ERK1/2 expression was not affected significantly while p-ERK1/2 and p-ERK/t-ERK ratio were significantly elevated in the Api co-treated group by 4.15 and 4.18 folds, respectively (Fig. 5A–D). Consequently, p-CREB, t-CREB levels, and p-CREB/t-CREB ratio were escalated by 1.5, 1.26, and 1.3 folds respectively in the hippocampus of Api co-treated rats compared with those in the MTX-alone group (Fig. 6A–C). Additionally, Api exerted a protective effect, raising the BDNF level to 1.24 times its level in the MTX group (Fig. 6D).

Api Co-treatment Attenuates the Microglial Activation Induced by MTX in the Rat Hippocampus

Iba-1 immunohistochemical staining has been considered an indicator for microglial activation. Iba-1 is a particular protein that plays a role in membrane ruffling and phagocytosis in activated microglia [34]. The effect of MTX and Api co-treatment is figured in Fig. 7A–D.

The area % of immunohistochemical expression of Iba-1 was significantly elevated in MTX rats by 2.05 folds compared with that in the normal control rats. On the other hand, administration of Api markedly decreased the Iba-1 expression by 41.63% compared with that in the MTX-alone treated rats (Fig. 7E).

Fig. 4 Effects of MTX and Api co-treatment on miR-15a/ROCK-1 levels in the rat hippocampus. Data are expressed as mean ± SD, $n = 6$. (**a**) significant difference from control, (**b**) significant difference from MTX. Significance level was set at $P < 0.05$. One-way ANOVA test and Tukey's post hoc test were used in the statistical analysis
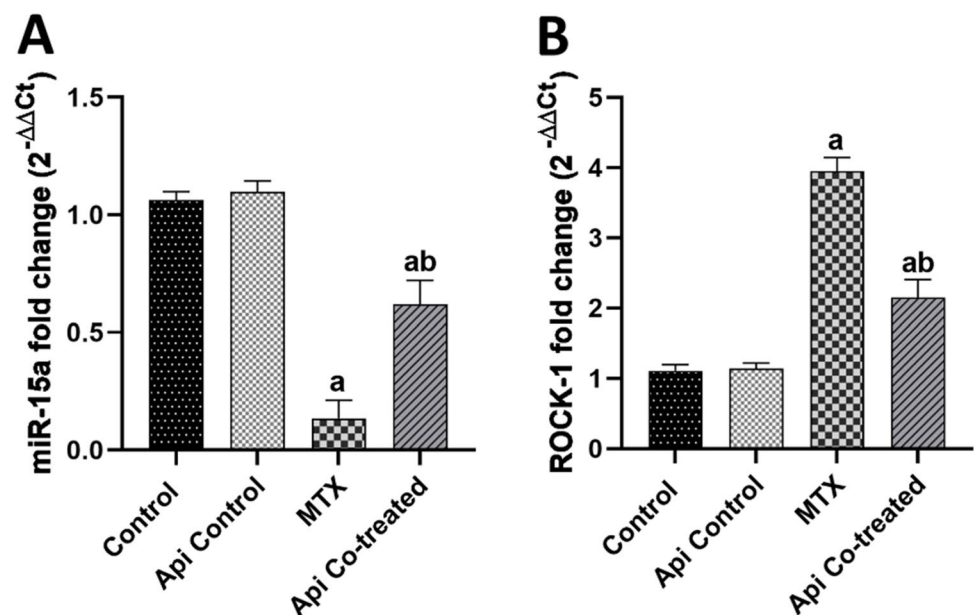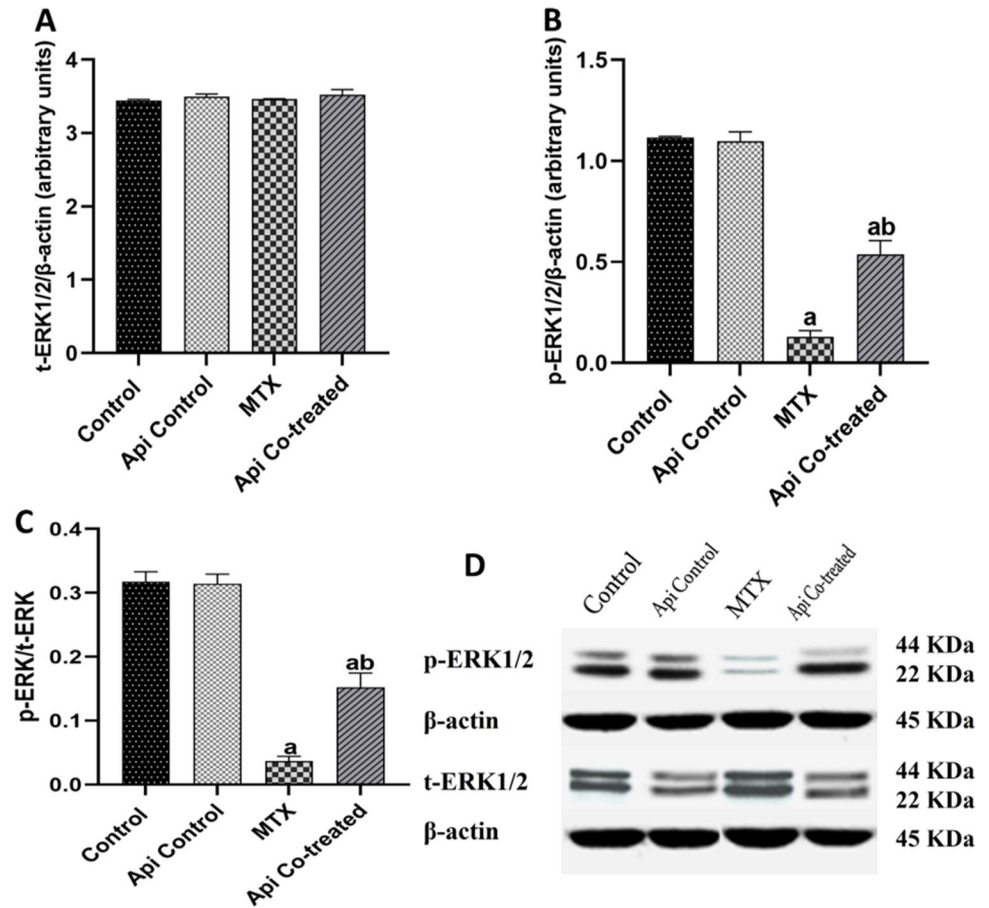
Api Abolishes the MTX-Induced Oxidative Stress, Neuroinflammation, and Apoptosis in the Rat Hippocampus

Both microglial activation and BDNF decline are known to induce oxidative stress, as evidenced by the recorded reduction of GSH levels by 38.05% along with elevation of MDA levels by 1.47 folds in the hippocampus of MTX-treated rats in comparison with levels in the control rats. Api administration throughout the study normalized the GSH and MDA levels, demonstrating its antioxidant capacity (Fig. 8A,B).

IL-1β levels were observed to increase by 1.53 folds in the hippocampal tissue following MTX treatment compared with those in the control rats. Enhanced apoptosis was also clear in the escalated hippocampal caspase-3 levels, which increased by 1.86 folds when compared with levels in the normal control rats. On the other hand, Api co-treatment counteracted these effects by inhibiting neuroinflammation and apoptosis, as evidenced by normalizing IL-1β and caspase-3 levels (Fig. 8C,D). Together, these

data accentuate the anti-inflammatory and antiapoptotic actions of Api.

Api Protects the Hippocampal DG and CA3 Regions Against Neuronal Degeneration Induced by MTX

Both normal and Api-control rats showed hippocampal layers with intact DG granule cells and a well-organized pyramidal neuron layer in CA3 with preserved nuclear and subcellular characteristics. MTX treatment exacerbated granule neuron degeneration in the DG and neuronal loss and shrinkage in CA3. In addition to intact-looking cells and perineuronal edema, the brain matrix had activated microglial cells. Api co-treated groups had more intact, well-organized granule cells with intact subcellular characteristics and higher chromatin condensation. Co-treatment with Api improved neuroprotective effectiveness, with fewer damaged or necrotic neurons and more intact, well-organized neurons. Mild persistent glial infiltrates were also seen (Fig. 9A–H).

Fig. 6 Effects of MTX and Api co-treatment on the CREB/BDNF protein expression. Data are expressed as mean ± SD, $n = 6$. (**a**) significant difference from control, (**b**) significant difference from MTX. Significance level was set at $P < 0.05$. One-way ANOVA test and Tukey's post hoc test were used in the statistical analysis
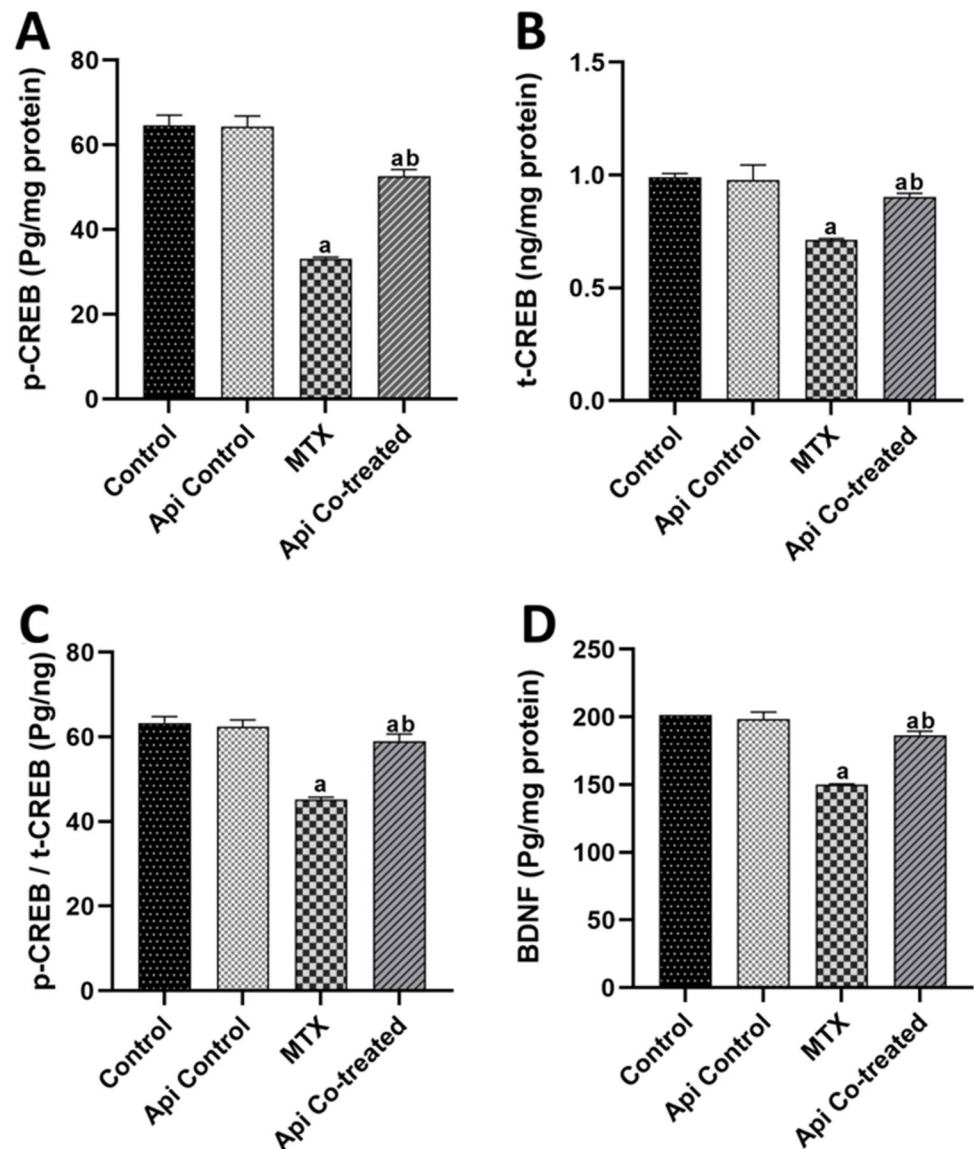
We further employed Nissl staining to detect degraded and intact neuron counts in DG and CA3 from all experimental groups (Fig. 9I–P). The intact neuron count in DG was recorded to decrease by 15.9% in MTX when compared with that in the normal control group. However, Api co-treatment was able to normalize the number of intact neurons (Fig. 9Q). In CA3, the intact neuron count was dramatically reduced in the MTX group in comparison with the decrease that occurred in the DG. Furthermore, Api co-treatment raised the intact neuron count by 5.77 folds compared with that in the MTX group (Fig. 9R).

Correlation Study

Several significant correlations between the various evaluated parameters are depicted in Fig. 10. miR-15a was positively correlated with ERK1/2/CREB/BDNF pathway parameters and GSH, and negatively correlated with ROCK-1, MDA, caspase-3, IL-1β, and Iba-1. ROCK-1 exhibited negative correlations with ERK1/2/CREB/BDNF and GSH, but it exhibited positive correlations with MDA, caspase-3, IL-1β, and Iba-1. All ERK1/2/CREB/BDNF pathway parameters showed similar significant correlation pattern, positively with GSH and negatively with MDA, caspase-3, and IL-1β. The microglial activation marker Iba-1 depicted substantial positive correlations with ROCK-1, MDA, caspase-3, and IL-1β, and significant negative correlations with miR-15a, ERK1/2/CREB/BDNF pathway parameters, and GSH ($P < 0.0001$ for all).

Discussion

The activation of microglia was one of the most recent hypotheses that were put forward to explain MTX-induced neurotoxicity [35]. To our knowledge, the

Fig. 7 Effect of MTX and Api co-treatment on microglial activation in the rat hippocampus. Data are expressed as mean ± SD, $n = 4$. (**a**) significant difference from control, (**b**) significant difference from MTX. Significance level was set at $P < 0.05$. One-way ANOVA test and Tukey's post hoc test were used in the statistical analysis. IHC, immunohistochemistry (**A–D** anti-Iba-1 immunostaining, 400×)
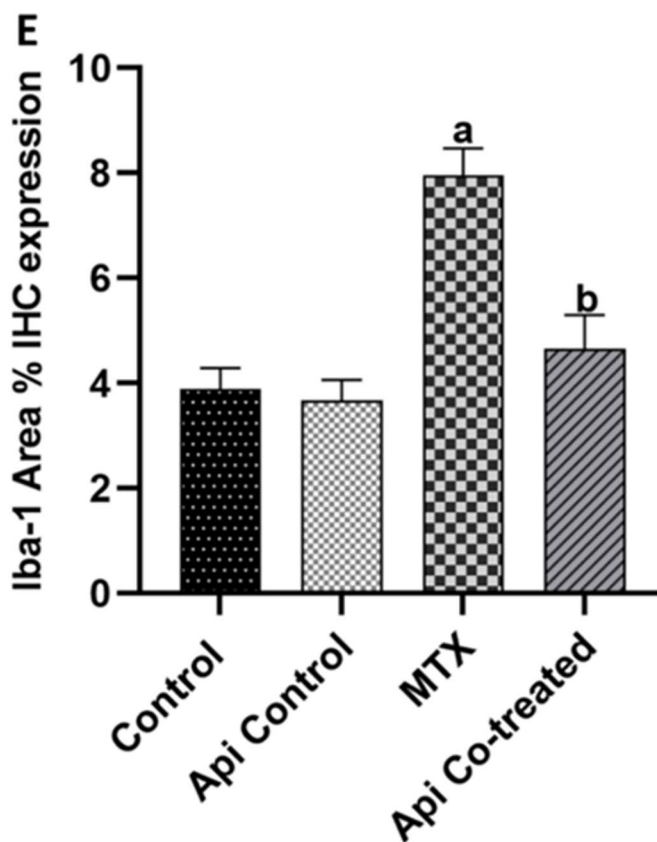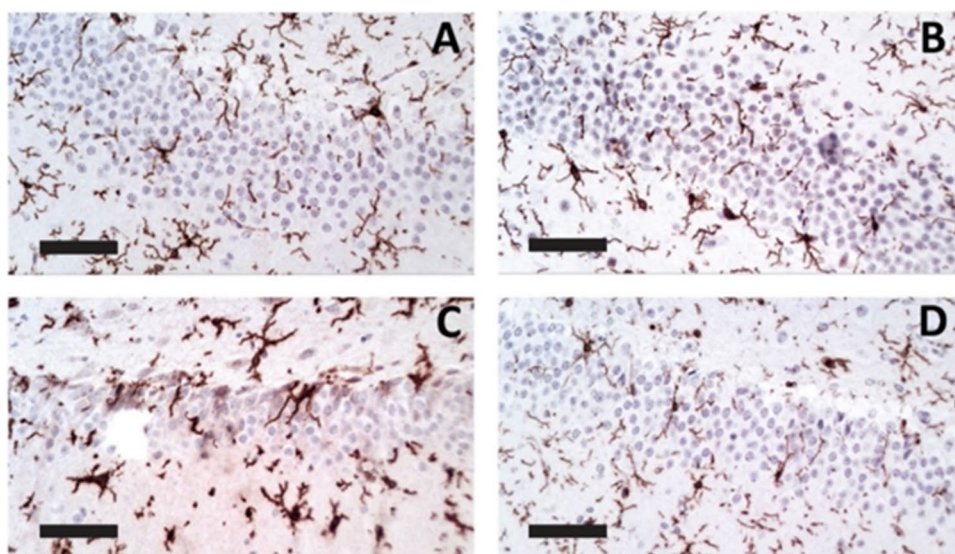
current study is the first to decipher the molecular underpinnings of MTX-induced microglial activation and to reveal that MTX mechanistically achieves this effect via downregulating miR-15a, raising the gene expression of its reported target ROCK-1, and subsequently decreasing the downstream p-ERK1/2, p-CREB, and BDNF levels in the rat hippocampus. This instigated microglial activation as evidenced by increased Iba-1 immunostaining,

ultimately incurring neuroinflammation, oxidative stress, and apoptosis, as shown by increased IL-1β, lipid peroxidation, and caspase-3 levels, respectively. Furthermore, this study is the first to provide evidence that Api mitigated the neurotoxicity of MTX by modulating the miR-15a/ROCK-1/ERK1/2/CREB/BDNF pathway, thereby in part reducing the microglial activation in the rats' hippocampi. These beneficial effects were concordant with

Fig. 8 Effects of MTX and Api co-treatment on oxidative stress, neuroinflammation, and apoptosis in the hippocampus. Data are expressed as mean ± SD, $n = 6$. (**a**) significant difference from control, (**b**) significant difference from MTX. Significance level was set at $P < 0.05$. One-way ANOVA test and Tukey's post hoc test were used in the statistical analysis
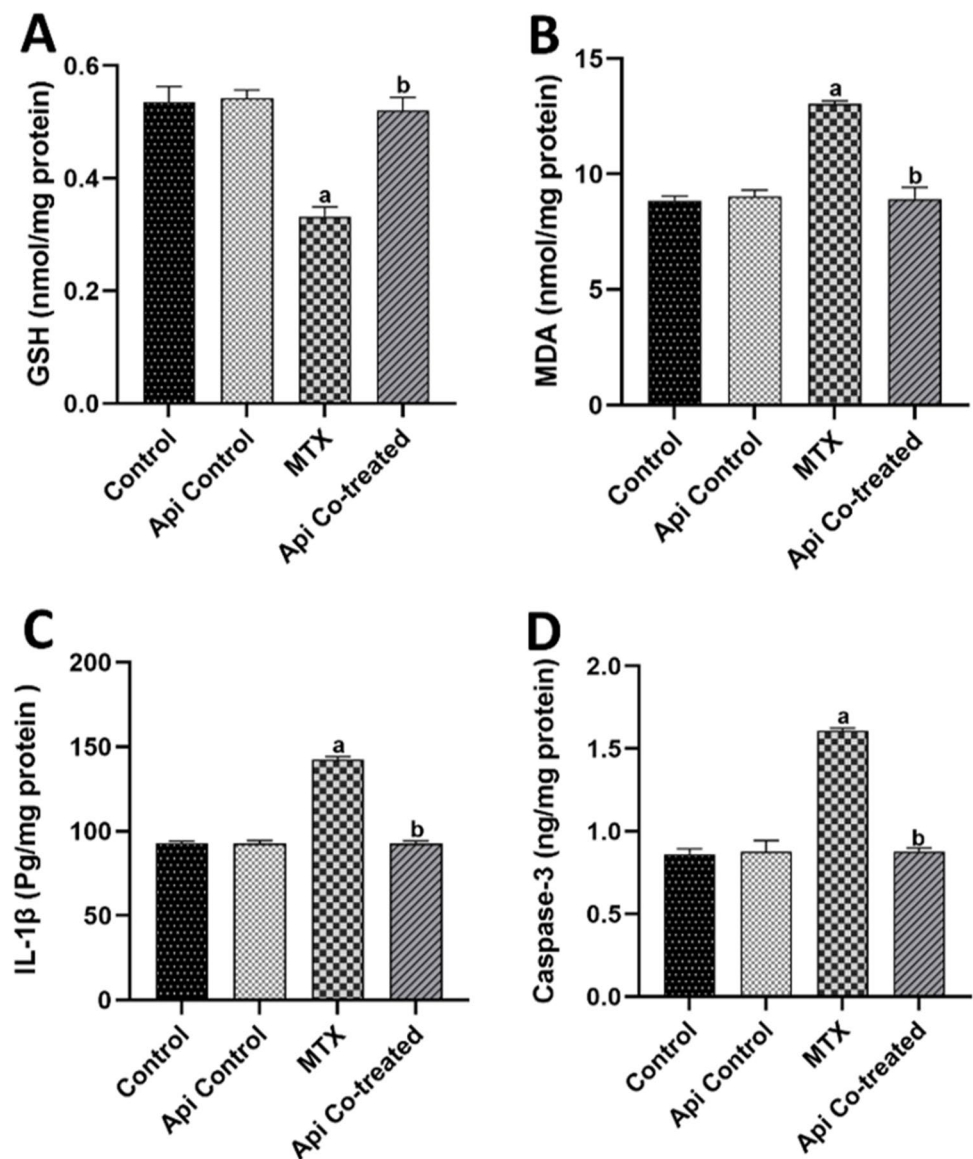
inhibition of neuroinflammation and apoptosis, restoration of the redox balance, and improvement in cognitive function, delineating its neuroprotective effects.

Herein, a considerable rise in Iba-1 immunohistochemical expression in the hippocampus of MTX-treated animals was observed along with increased glial cell infiltrates in the DG and CA3 hippocampal regions, indicating heightened microglial activation. These findings were in line with the growing evidence associating MTX with microglial activation [6, 36, 37]. Recent data highlighted heightened activation of the microglia to be a cause of neurodegenerative diseases including AD, parkinsonism, and frontotemporal dementia [38–40]. Microglial stimulation is known to create reactive astrocytes that affect the normal function of neurons and is thought to be involved in neurodegenerative disorders [41–43]. The microglia are CNS-resident macrophages, and it has been demonstrated that microglia with both M1 and M2 phenotypes play a dual role in most neurodegenerative diseases. M1 is a proinflammatory cell that induces the generation of reactive oxygen species and IL-1β, whereas M2 is an anti-inflammatory cell [44]. To note, MTX was shown to induce chronic microglial activation and subsequent derangements that were dependent on the inflammatory microglia [6]. Our data are in line with M1 phenotype activation, confirmed by the observed histopathological alterations and the neuroinflammatory status evidenced by elevated levels of IL-1β in the hippocampus of MTX-treated rats.

In this study, we elaborated on the molecular mechanism underlying the microglial activation induced by MTX. Given that the link between ROCK-1 induction and microglial activation was reported [45], we explored the effect

of MTX on ROCK-1 as a possible mediator and further expatiated its upstream and downstream effectors. Our data revealed upregulation of ROCK-1 along with downregulation of its upstream effector miR-15a and reduction of its downstream target ERK1/2 in the hippocampi of rats treated with MTX. Indeed, previous data has associated ROCK-1 upregulation with various neurodegenerative disorders, including AD [12, 46]. Furthermore, miR-15a downregulation, upstream of ROCK-1, was previously associated with AD [47]. Herein, miR-15a was dramatically downregulated in the hippocampus of MTX-treated rats, supporting the previous findings which correlated the downregulation of miR-15a with the overexpression of ROCK-1 [18, 48]. ROCK-1 activation has been lately proven to have a role in mediating neuroinflammation via directly evoking microglial activation through increasing M1 neuroinflammatory phenotype size and count [49, 50] or indirectly via the effect of ROCK-1 on ERK1/2/CREB/ BDNF pathway [51, 52]. This was proven by the observed negative correlations between ROCK-1 and miR-15a as well as ERK1/2/CREB/BDNF pathway parameters.

ROCK-1 has been proven to negatively affect ERK1/2 activation [53]. Notably, we found a significant decline of activated ERK (p-ERK1/2) manifested by the reduced p-ERK/t-ERK ratio in the hippocampus of the MTX-alone group. In our study, p-ERK1/2 showed a direct relation with CREB phosphorylation, with a decline in activated CREB (p-CREB) as well as p-CREB/t-CREB ratio was noticed in the hippocampus of the MTX-treated group. We recorded a significant decline in BDNF levels downstream of CREB due to MTX injections. These results support the previous data reporting that decreased CREB/BDNF axis results in impaired neurogenesis and neuroinflammation as well as neuronal survival [16, 48, 54].

Interestingly, microglial activation was shown to perpetuate the decline in BDNF levels, resulting in cognitive impairment [8]. Indeed, microglial activation invokes an imbalance between proinflammatory and anti-inflammatory cytokines and prompts a reduction in cell proliferation and BDNF levels, leading to activation of apoptosis, reduced hippocampal neurogenesis, and spatial memory loss [7]. BDNF is one of the most important neurotrophins regulating brain homeostasis. Hippocampal BDNF enhances neuronal survival, neuroplasticity, and neurogenesis, preserving learning, memory, and cognitive functions of the brain. BDNF binds to the tyrosine kinase B receptor (TrkB) activating neuroprotective pathways, including the ERK1/2/ CREB pathway, which itself upregulates BDNF [40, 55].

Compelling data suggest that microglial activation as well as decreased CREB/BDNF to be important activators

for oxidative stress and inflammatory cytokines in AD, autism, and neurodegenerative disease, leading to cognitive and learning impairment [7, 56–58]. Moreover, earlier research has linked microglial activation, IL-1β elevation, and BDNF reduction to anesthesia- and surgery-induced hippocampus cognitive impairment [59]. In this context, MTX was found to have neuroinflammatory side effects through provoking oxidative stress and a proinflammatory milieu. Eliciting oxidative stress by MTX in the rat hippocampi led to an increase in the inflammatory mediator IL-1β and the apoptotic marker caspase-3. This was evidenced by the observed decrease in GSH levels, elevation of lipid peroxidation, and a marked increase in IL-1β levels in the hippocampus. A mechanistic explanation of the increased neuroinflammation could be based on ROCK-1-mediated microglial activation through an altered miR-15a/ROCK-1/ERK1/2/CREB/BDNF pathway.

Our findings from the correlation analysis implied elevated expression of ROCK-1 to increase oxidative stress and proinflammatory markers, leading to activated apoptosis and neural death. This supports the data of a recent study that has associated ROCK-1 activation with increased inflammatory cytokines in the hippocampus, which leads to neuronal death and cognitive dysfunction [10]. Caspase-3 which is an important protease in the apoptosis process was found to increase in the MTX group, which indicates that MTX is a neuro-lethal drug. This data was also supported by the histopathological examination of the hippocampus, which revealed higher records of degenerated granule neurons in the MTX group hippocampi. Furthermore, Nissl staining showed a significant decrease in intact neurons in both DG and CA3. Therefore, our results spotlight that both activation of microglia and downregulation of BDNF by MTX are possible mechanisms that underlie the neuroinflammatory apoptotic consequences.

Our behavioral analysis data showed a significant decline in the learning ability and cognitive function due to MTX treatment. These data came in line with recently reported data linking MTX administration to an increased risk of cognitive impairment and memory problems in juvenile patients, resulting in an impaired learning outcome [60]. In the performed NOR test, the MTX group showed a negative discrimination index and lower preference index, which means that the rats were totally unable to discriminate between old and novel objects during the choice trial. The conducted MWM test came up with a similar observation, which revealed a dramatic elevation in the escaping latency of the MTX-treated rats in addition to a substantial decrease in both the quadrant time and path efficiency of the probe test. Our data support previous reports
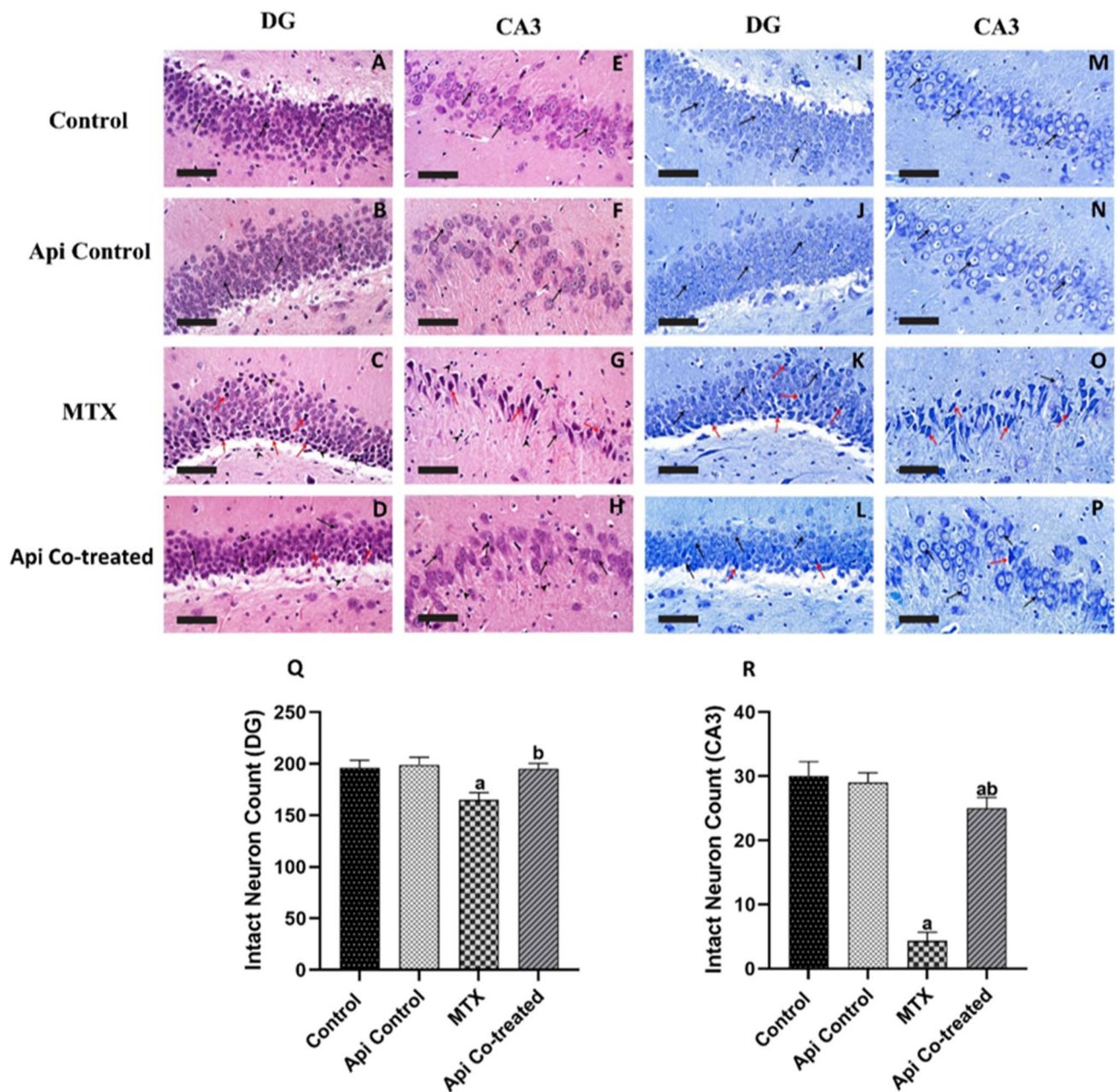
suggesting a negative correlation between BDNF levels and escape latency [61] as well as elevation of escape latency in microglial activation models [62].

Our work further contemplated the neuroprotective effect of Api on MTX-induced neurodegeneration. Recent growing data highlighted Api as a neuroprotective naturally occurring flavonoid in parkinsonism [63], methylmercury neurotoxicity [64], and depressive disorders [65]. In particular, Api was studied for its neuroprotective action in various models due to its antioxidant and anti-inflammatory activity [65, 66]. In our study, Api co-treatment proved itself as a potential antidote for MTX-induced neuroinflammation, attenuating its neurotoxicity. The Api co-treated group showed a 4.63-fold elevation in

the gene expression of miR-15a and a substantial reduction in ROCK-1 expression. Consequently, microglial activation was mitigated as shown by the substantial decline in Iba-1 levels in the hippocampus of the Api co-treated group, reaching 58.37% of levels in the MTX-alone group. Similarly, a previous study demonstrated that Api inhibits M1 microglia [65]. Furthermore, Api has been reported to have an inhibitory action on microglial inflammatory effects in cultured microglia and in in vitro models of neuroinflammation associated with AD [21, 67]. Moreover, recent data highlighted the indirect inhibitory effect of Api on ROCK-1 expression in hepatocellular carcinoma models in vivo and in vitro [68] as well as the upregulatory effect on BDNF in kindled mice models [19]. Taken together, these data

◄**Fig. 9** Histopathological effects of MTX and Api co-treatment in the DG and CA3 regions of the hippocampus. **A–D** DG H&E stain. **E–H** CA3 H&E stain. **A** Normal control and **B** Api control, both demonstrated normal morphological features of hippocampal layers in the DG region, including granule cells at different zones with intact subcellular details (arrow) as well as hilar region without abnormal alterations. **C** MTX treatment increased degenerated granule neurons and nuclear pyknosis (red arrow). Moderate edema accompanied by mild higher reactive glial cells infiltrates (arrowhead). **D** Api co-treatment showed markedly higher neuroprotective effects with several images of intact granule cells with intact subcellular features and increased chromatin condensation (black arrow). Few sporadic degenerated neurons (red arrow) with minor glial infiltration were seen. **E** Normal control and **F** Api control, both demonstrated normal morphological structures of hippocampal layers in CA3 region with apparent intact well-organized pyramidal neurons with intact nuclear and subcellular details (black arrow). Intact intercellular matrix was observed with minimal reactive glial cells infiltration. **G** MTX treated, showed severe neuronal loss and abundant records of hyperesenophilic, angular necrotic pyramidal neurons without distinct subcellular details (red arrow) alternated with few scattered apparent intact cells (black arrow), mild perineuronal edema were shown in brain matrix with marked higher reactive microglial cell infiltrates (arrowhead). **H** Api co-treated demonstrated much superior neuroprotective efficacy with sporadic few deteriorated or necrotic neurons (red arrow) and significantly higher figures of intact well-organized neurons (black arrow). Mild persistent reactive glial cell infiltrates were shown (arrowhead). **I–P** Nissl staining of DG and CA3 to detect intact (black arrow) and damaged (red arrow) neurons. **Q** Intact neurons count in DG. **R** Intact neurons count in CA3 area. Data are expressed as mean ± SD, $n = 4$. (a) significant difference from control, (b) significant difference from MTX. Significance level was set at $P < 0.05$. One-way ANOVA test and Tukey's post hoc test were used in the statistical analysis. **A–D** H&E 400×, **E–H** H&E 1000×, **I–L** Nissl staining 400×, **M–P** Nissl staining 1000×

support that ROCK-1 inhibition by Api could be neuroprotective against MTX-induced derangements in the rat brain.

Our results further elucidated the molecular mechanisms of the Api neuroprotective effects of ROCK-1 inhibition. Api seems to activate the ERK1/2/CREB/BDNF pathway, attested by elevated p-ERK1/2, p-CREB, and BDNF levels in the rats' hippocampi. Concurrently, elevation of GSH and decrements in lipid peroxidation, IL-1β, and caspase-3 levels were proven by our analysis of inflammatory, oxidative, and apoptotic markers in the hippocampus of Api co-treated rats. These results are in alignment with previously published data that Api reduced oxidative stress and inhibited apoptosis in various models, including doxorubicin-induced cardiotoxicity [69] and parkinsonism [63]. Furthermore, previous studies demonstrated similar results for Api on GSH, MDA, and IL-1β [70]. Thus, one can speculate that both inhibition of microglial activation and ERK1/2/CREB/BDNF pathway activation potentiate the anti-inflammatory, antioxidant, and antiapoptotic effects of Api in this model. These protective effects explain the increased neuronal survival and neuroplasticity in the hippocampi of Api co-treated rats, showing higher intact neuron count in both DG and CA3 regions. This was reflected in the substantial improvement in cognitive and

learning behavior manifested by increments in the discriminating index in NOR and the escape delay in MWM.

Our findings emphasized the impact of ROCK-1 inhibition as a possible target for attenuating MTX-induced neuroinflammation. This was consistent with previous studies that highlighted ROCK-1 inhibition as an important player in neuroprotection and inhibiting neuroinflammation via multiple mechanisms, such as decreasing both microglial activation and oxidative stress by shifting between M1 and M2 microglia phenotypes, inhibiting apoptosis [12], and its effect on activating the ERK1/2/CREB/BDNF neuroprotective pathway [51]. Api suppressed ROCK-1, reduced microglial activation, neuroinflammation, oxidative stress, and apoptosis, establishing itself as a promising co-treatment for mitigating MTX-induced neurotoxicity. This work has noteworthy limitations, and we urge that future research focus on studying the effect of different MTX and Api doses. Furthermore, research potential miRNAs and other neurotrophic factors that may be influenced by the pathways investigated in this study.

Conclusion

MTX-induced neurotoxicity and cognitive impairment could be attributed to the microglial activation and neuroinflammatory response in part through the miR-15a/ROCK-1/ERK1/2/CREB/BDNF cascade. This study advocates the neuroprotective effects of Api through its
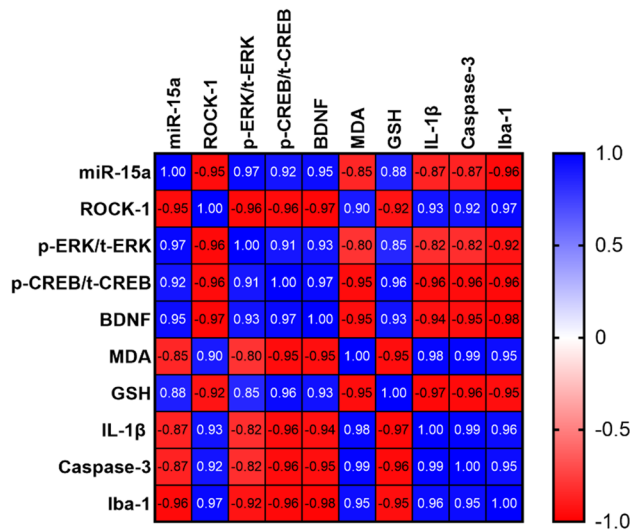

Fig. 10 Heatmap of the correlation matrix between different biochemical and immunohistochemical parameters in all studied groups. Values are expressed as the Pearson r correlation coefficient, with statistical significance $P < 0.0001$ for all correlations. For each parameter, data from all studied groups were included, $n = 24$, except Iba-1 $n = 16$
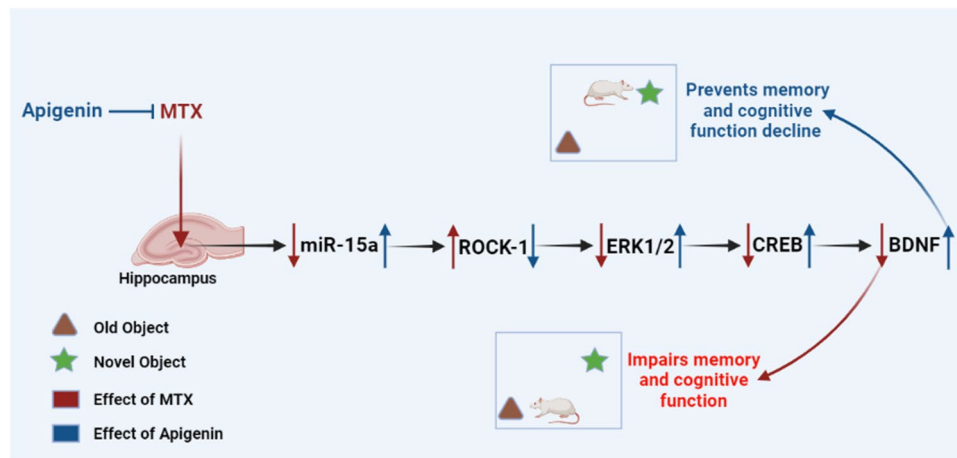
Fig. 11 Summative illustrative graph for the study results. MTX administration resulted in the downregulation of hippocampal miR-15a, which induced an increase in the expression of its target ROCK-1, hence blocking the downstream ERK1/2/CREB/BDNF pathway and causing memory loss and cognitive impairment. Api co-treatment, on the other hand, mitigated the MTX effects by restoring miR-15a, reducing ROCK-1 expression, and activating the ERK1/2/CREB/BDNF pathway, resulting in enhanced memory and cognitive function in MTX-treated rats

inhibitory effect on MTX-induced microglial activation, along with lessening neuroinflammation, oxidative stress, and apoptosis, and boosting the cognitive function of rats via possible modulation of the miR-15a/ROCK-1/ERK1/2/CREB/BDNF pathway in the hippocampus. Our findings lay the groundwork that Api could serve as a considerable option for attenuating MTX-induced neuroinflammation and neurotoxicity. A summary of the current results is presented in Fig. 11.

Data Availability The datasets used and analyzed during the current study are available upon reasonable request from the corresponding author.

Declarations

Ethics Approval and Consent to Participate The Research Ethics Committee for Experimental and Clinical Studies, Faculty of Pharmacy, Cairo University, Cairo, Egypt, authorized all animal procedures and experimental protocols (Permit Number: BC2944).

Consent of Publication Not applicable.

Competing Interests The authors declare no competing interests.

References

1. Youssef AA, Raafat TA, Madney Y (2015) Child with acute methotrexate related neurotoxicity: can diffusion weighted MRI help?? Egypt J Radiol Nucl Med 46(4):1149–1153

2. Krull KR, Hardy KK, Kahalley LS, Schuitema I, Kesler SR (2018) Neurocognitive outcomes and interventions in long-term survivors of childhood cancer. J Clin Oncol 36(21):2181

3. Rijmenams I, Moechars D, Uyttebroeck A, Radwan A, Blommaert J, Deprez S, Sunaert S, Segers H et al (2021) Age-and intravenous methotrexate-associated leukoencephalopathy and its neurological impact in pediatric patients with lymphoblastic leukemia. Cancers 13(8):1939

4. Welbat JU, Naewla S, Pannangrong W, Sirichoat A, Aranarochana A, Wigmore PJBP (2020) Neuroprotective effects of hesperidin against methotrexate-induced changes in neurogenesis and oxidative stress in the adult rat. Biochem Pharmacol 178:114083. https://doi.org/10.1016/j.bcp.2020.114083

5. Wen J, Patel C, Diglio F, Baker K, Marshall G, Li S, Cole PD (2022) Cognitive impairment persists at least 1 year after juvenile rats are treated with methotrexate. Neuropharmacology 206:108939

6. Gibson EM, Nagaraja S, Ocampo A, Tam LT, Wood LS, Pallegar PN, Greene JJ, Geraghty AC et al (2019) Methotrexate chemotherapy induces persistent tri-glial dysregulation that underlies chemotherapy-related cognitive impairment. Cell 176(1):43–55. https://doi.org/10.1016/j.cell.2018.10.049

7. Wadhwa M, Prabhakar A, Ray K, Roy K, Kumari P, Jha PK, Kishore K, Kumar S et al (2017) Inhibiting the microglia activation improves the spatial memory and adult neurogenesis in rat hippocampus during 48 h of sleep deprivation. J Neuroinflammation 14(1):1–18

8. Geraghty AC, Gibson EM, Ghanem RA, Greene JJ, Ocampo A, Goldstein AK, Ni L, Yang T et al (2019) Loss of adaptive myelination contributes to methotrexate chemotherapy-related cognitive impairment. Neuron 103(2):250–265

9. Seigers R, Timmermans J, van der Horn HJ, de Vries EF, Dierckx RA, Visser L, Schagen SB, van Dam FS et al (2010) Methotrexate reduces hippocampal blood vessel density and activates microglia in rats but does not elevate central cytokine release. Behav Brain Res 207(2):265–272

10. Lee EC, Hong D-Y, Lee D-H, Park S-W, Lee JY, Jeong JH, Kim E-Y, Chung H-M et al (2022) Inflammation and rho-associated protein kinase-induced brain changes in vascular dementia. Biomedicines 10(2):446

11. Henderson BW, Gentry EG, Rush T, Troncoso JC, Thambisetty M, Montine TJ, Herskowitz JH (2016) Rho-associated protein kinase 1 (ROCK 1) is increased in Alzheimer's disease and ROCK 1 depletion reduces amyloid-β levels in brain. J Neurochem 138(4):525–531

12. Koch JC, Tatenhorst L, Roser A-E, Saal K-A, Tönges L, Lingor P (2018) ROCK inhibition in models of neurodegeneration and its potential for clinical translation. Pharmacol Ther 189:1–21

13. Borrajo A, Rodriguez-Perez AI, Diaz-Ruiz C, Guerra MJ, Labandeira-Garcia JL (2014) Microglial TNF-α mediates enhancement of dopaminergic degeneration by brain angiotensin. Glia 62(1):145–157

14. Barcia C, Ros CM, Annese V, Carrillo-de Sauvage MA, Ros-Bernal F, Gómez A, Yuste JE, Campuzano CM et al (2012) ROCK/Cdc42-mediated microglial motility and gliapse formation lead to phagocytosis of degenerating dopaminergic neurons in vivo. Sci Rep 2(1):1–13

15. Ding J, Li QY, Wang X, Sun CH, Lu CZ, Xiao BG (2010) Fasudil protects hippocampal neurons against hypoxia-reoxygenation injury by suppressing microglial inflammatory responses in mice. J Neurochem 114(6):1619–1629

16. Hensel N, Rademacher S, Claus P (2015) Chatting with the neighbors: crosstalk between Rho-kinase (ROCK) and other signaling pathways for treatment of neurological disorders. Front Neurosci 9:198

17. Yang S, Wang G, Ma ZF, Lq Q, Zhai Yj YuZL, Xue M, Zhang Yh, Wan Z (2020) Dietary advanced glycation end products–induced cognitive impairment in aged ICR mice: protective role of quercetin. Mol Nutr Food Res 64(3):1901019

18. Li X, Wang S-W, Li X-L, Yu F-Y, Cong H-M (2020) Knockdown of long non-coding RNA TUG1 depresses apoptosis of hippocampal neurons in Alzheimer's disease by elevating microRNA-15a and repressing ROCK1 expression. Inflamm Res 69(9):897–910

19. Sharma P, Sharma S, Singh D (2020) Apigenin reverses behavioural impairments and cognitive decline in kindled mice via CREB-BDNF upregulation in the hippocampus. Nutr Neurosci 23(2):118–127

20. Han J-Y, Ahn S-Y, Kim C-S, Yoo S-K, Kim S-K, Kim H-C, Hong JT, Oh K-W (2012) Protection of apigenin against kainate-induced excitotoxicity by anti-oxidative effects. Biol Pharm Bull 35(9):1440–1446

21. Dourado NS, Souza CdS, De Almeida MMA, Bispo da Silva A, Dos Santos BL, Silva VDA, De Assis AM, da Silva JS et al (2020) Neuroimmunomodulatory and neuroprotective effects of the flavonoid apigenin in in vitro models of neuroinflammation associated with Alzheimer's disease. Front Aging Neurosci 12:119

22. Sirichoat A, Krutsri S, Suwannakot K, Aranarochana A, Chaisawang P, Pannangrong W, Wigmore P, Welbat JU (2019) Melatonin protects against methotrexate-induced memory deficit and hippocampal neurogenesis impairment in a rat model. Biochem Pharmacol 163:225–233

23. Sritawan N, Prajit R, Chaisawang P, Sirichoat A, Pannangrong W, Wigmore P, Welbat JU (2020) Metformin alleviates memory and hippocampal neurogenesis decline induced by methotrexate chemotherapy in a rat model. Biomed Pharmacother 131:110651

24. Naewla S, Sirichoat A, Pannangrong W, Chaisawang P, Wigmore P, Welbat JU (2019) Hesperidin alleviates methotrexate-induced memory deficits via hippocampal neurogenesis in adult rats. Nutrients 11(4):936

25. Fayez AM, Mansour DF, Saleh DO (2021) Progression of hepatic encephalopathy induced by bile duct ligation versus thioacetamide in rats: regulatory role of apigenin. J Appl Pharm Sci 11(12):158–168

26. Malik S, Suchal K, Khan SI, Bhatia J, Kishore K, Dinda AK, Arya DS (2017) Apigenin ameliorates streptozotocin-induced diabetic nephropathy in rats via MAPK-NF-κB-TNF-α and TGF-β1-MAPK-fibronectin pathways. Am J Physiol Renal Physiol 313(2):F414–F422

27. Antunes M, Biala G (2012) The novel object recognition memory: neurobiology, test procedure, and its modifications. Cogn Process 13(2):93–110

28. Broadbent NJ, Squire LR, Clark RE (2004) Spatial memory, recognition memory, and the hippocampus. Proc Natl Acad Sci 101(40):14515–14520

29. Gehring TV, Luksys G, Sandi C, Vasilaki E (2015) Detailed classification of swimming paths in the Morris water maze: multiple strategies within one trial. Sci Rep 5(1):1–15

30. Motawi TK, El-Maraghy SA, Sabry D, Nady OM, Senousy MA (2022) Cromolyn chitosan nanoparticles reverse the DNA methylation of RASSF1A and p16 genes and mitigate DNMT1 and METTL3 expression in breast cancer cell line and tumor xenograft model in mice. Chem Biol Interact 365:110094. https://doi.org/10.1016/j.cbi.2022.110094

31. Culling CFA (2013) Handbook of histopathological and histochemical techniques: including museum techniques. Butterworth-Heinemann

32. Abbas H, Gad HA, Khattab MA, Mansour M (2021) The tragedy of Alzheimer's disease: towards better management via resveratrol-loaded oral bilosomes. Pharmaceutics 13(10):1635

33. Schneider CA, Rasband WS, Eliceiri KW (2012) NIH Image to ImageJ: 25 years of image analysis. Nat Methods 9(7):671–675. https://doi.org/10.1038/nmeth.2089

34. Desale SE, Chinnathambi S (2021) α-Linolenic acid induces clearance of tau seeds via actin-remodeling in microglia. Mol Biomed 2(1):1–14

35. Chen Y-C, Sheen J-M, Wang S-C, Hsu M-H, Hsiao C-C, Chang K-A, Huang L-T (2021) Methotrexate neurotoxicity is related to epigenetic modification of the myelination process. Int J Mol Sci 22(13):6718

36. Vazi E, Holanda F, Santos N, Cardoso C, Martins M, Bondan E (2021) Short-term systemic methotrexate administration in rats induces astrogliosis and microgliosis. Res Vet Sci 138:39–48

37. Gibson EM, Monje M (2021) Microglia in cancer therapy-related cognitive impairment. Trends Neurosci 44(6):441–451

38. Bachiller S, Jiménez-Ferrer I, Paulus A, Yang Y, Swanberg M, Deierborg T, Boza-Serrano A (2018) Microglia in neurological diseases: a road map to brain-disease dependent-inflammatory response. Front Cell Neurosci 12:488

39. Motawi TK, Al-Kady RH, Abdelraouf SM, Senousy MA (2022) Empagliflozin alleviates endoplasmic reticulum stress and augments autophagy in rotenone-induced Parkinson's disease in rats: targeting the GRP78/PERK/eIF2α/CHOP pathway and miR-211-5p. Chem Biol Interact 362:110002

40. Liu S, Fan M, Xu J-X, Yang L-J, Qi C-C, Xia Q-R, Ge J-F (2022) Exosomes derived from bone-marrow mesenchymal stem cells alleviate cognitive decline in AD-like mice by improving BDNF-related neuropathology. J Neuroinflammation 19(1):1–20

41. Siracusa R, Fusco R, Cuzzocrea S (2019) Astrocytes: role and functions in brain pathologies. Front Pharmacol 10:1114

42. Motawi TK, Al-Kady RH, Senousy MA, Abdelraouf SM (2023) Repaglinide elicits a neuroprotective effect in rotenone-induced Parkinson's disease in rats: emphasis on targeting the DREAM-ER stress BiP/ATF6/CHOP trajectory and activation of mitophagy. ACS Chem Neurosci 14(1):180–194. https://doi.org/10.1021/acschemneuro.2c00656

43. Liddelow SA, Guttenplan KA, Clarke LE, Bennett FC, Bohlen CJ, Schirmer L, Bennett ML, Münch AE et al (2017) Neurotoxic reactive astrocytes are induced by activated microglia. Nature 541(7638):481–487

44. Tang Y, Le W (2016) Differential roles of M1 and M2 microglia in neurodegenerative diseases. Mol Neurobiol 53(2):1181–1194

45. Shinozaki Y, Danjo Y, Koizumi S (2019) Microglial ROCK is essential for chronic methylmercury-induced neurodegeneration. J Neurochem 151(1):64–78

46. Hu Y-B, Zou Y, Huang Y, Zhang Y-F, Lourenco GF, Chen S-D, Halliday GM, Wang G et al (2016) ROCK1 is associated with Alzheimer's disease-specific plaques, as well as enhances autophagosome formation but not autophagic Aβ clearance. Front Cell Neurosci 10:253

47. Hébert SS, Papadopoulou AS, Smith P, Galas M-C, Planel E, Silahtaroglu AN, Sergeant N, Buée L et al (2010) Genetic ablation of Dicer in adult forebrain neurons results in abnormal tau hyperphosphorylation and neurodegeneration. Hum Mol Genet 19(20):3959–3969

48. Taha M, Eldemerdash OM, Elshaffei IM, Yousef EM, Senousy MA (2023) Dexmedetomidine attenuates methotrexate-induced neurotoxicity and memory deficits in rats through improving hippocampal neurogenesis: the role of miR-15a/ROCK-1/ERK1/2/CREB/BDNF pathway modulation. Int J Mol Sci 24(1):766. https://doi.org/10.3390/ijms24010766

49. Ren Y, Li H, Xie W, Wei N, Liu M (2019) MicroRNA-195 triggers neuroinflammation in Parkinson's disease in a Rho-associated kinase 1-dependent manner. Mol Med Rep 19(6):5153–5161

50. Wang Q, Song L-J, Ding Z-B, Chai Z, Yu J-Z, Xiao B-G, Ma C-G (2022) Advantages of Rho-associated kinases and their inhibitor fasudil for the treatment of neurodegenerative diseases. Neural Regen Res 17(12):2623–2631

51. Wu H, Wang M, Li X, Shao Y (2021) The metaflammatory and immunometabolic role of macrophages and microglia in diabetic retinopathy. Hum Cell 34(6):1617–1628

52. Liu B, Zhang Y, Yang Z, Liu M, Zhang C, Zhao Y, Song C (2021) ω-3 DPA protected neurons from neuroinflammation by balancing microglia M1/M2 polarizations through inhibiting NF-κB/MAPK p38 signaling and activating neuron-BDNF-PI3K/AKT pathways. Mar Drugs 19(11):587

53. Li F, Jiang Q, Shi K, Luo H, Yang Y, Xu C (2013) RhoA modulates functional and physical interaction between ROCK1 and Erk1/2 in selenite-induced apoptosis of leukaemia cells. Cell Death Dis 4(7):e708–e708

54. Ying S-W, Futter M, Rosenblum K, Webber MJ, Hunt SP, Bliss TV, Bramham CR (2002) Brain-derived neurotrophic factor induces long-term potentiation in intact adult hippocampus: requirement for ERK activation coupled to CREB and upregulation of Arc synthesis. J Neurosci 22(5):1532–1540

55. Minichiello L (2009) TrkB signalling pathways in LTP and learning. Nat Rev Neurosci 10(12):850–860

56. Kumar H, Diwan V, Sharma B (2022) Remediate effect of ryanodine receptor antagonist in valproic-acid induced autism. Biomed Pharmacol J 15(1):59–71

57. Chen J-H, Ke K-F, Lu J-H, Qiu Y-H, Peng Y-P (2015) Protection of TGF-β1 against neuroinflammation and neurodegeneration in Aβ1–42-induced Alzheimer's disease model rats. PLoS ONE 10(2):e0116549

58. Prakash A, Kumar A (2014) Role of nuclear receptor on regulation of BDNF and neuroinflammation in hippocampus of β-amyloid animal model of Alzheimer's disease. Neurotox Res 25(4):335–347

59. Qiu L-L, Pan W, Luo D, Zhang G-F, Zhou Z-Q, Sun X-Y, Yang J-J, Ji M-H (2020) Dysregulation of BDNF/TrkB signaling mediated by NMDAR/Ca2+/calpain might contribute to postoperative cognitive dysfunction in aging mice. J Neuroinflammation 17(1):1–15

60. Wen J, Maxwell RR, Wolf AJ, Spira M, Gulinello ME, Cole PD (2018) Methotrexate causes persistent deficits in memory and executive function in a juvenile animal model. Neuropharmacology 139:76–84

61. Fathi D, Abulsoud AI, Saad MA, Nassar NN, Maksimos MM, Rizk SM, Senousy MA (2021) Agomelatine attenuates alcohol craving and withdrawal symptoms by modulating the Notch1 signaling pathway in rats. Life Sci 284:119904

62. Sacher C, Blume T, Beyer L, Peters F, Eckenweber F, Sgobio C, Deussing M, Albert NL et al (2019) Longitudinal PET monitoring of amyloidosis and microglial activation in a second-generation amyloid-β mouse model. J Nucl Med 60(12):1787–1793

63. Patel M, Singh S (2022) Apigenin attenuates functional and structural alterations via targeting NF-kB/Nrf2 signaling pathway in LPS-induced parkinsonism in experimental rats. Neurotox Res 40:941–960

64. Yadav RK, Mehan S, Sahu R, Kumar S, Khan A, Makeen HA, Al Bratty M (2022) Protective effects of apigenin on methylmercury-induced behavioral/neurochemical abnormalities and neurotoxicity in rats. Hum Exp Toxicol 41:1–20. https://doi.org/10.1177/09603271221084276

65. Bijani S, Dizaji R, Sharafi A, Hosseini M-J (2022) Neuroprotective effect of apigenin on depressive-like behavior: mechanistic approach. Neurochem Res 47(3):644–655

66. Nabavi SF, Khan H, D'onofrio G, Šamec D, Shirooie S, Dehpour AR, Argüelles S, Habtemariam S et al (2018) Apigenin as neuroprotective agent: of mice and men. Pharmacol Res 128:359–365

67. Rezai-Zadeh K, Ehrhart J, Bai Y, Sanberg PR, Bickford P, Tan J, Shytle RD (2008) Apigenin and luteolin modulate microglial activation via inhibition of STAT1-induced CD40 expression. J Neuroinflammation 5(1):1–10

68. Wang S-M, Yang P-W, Feng X-J, Zhu Y-W, Qiu F-J, Hu X-D, Zhang S-H (2021) Apigenin inhibits the growth of hepatocellular carcinoma cells by affecting the expression of microRNA transcriptome. Front Oncol 11:657665. https://doi.org/10.3389/fonc.2021.657665

69. Zare MFR, Rakhshan K, Aboutaleb N, Nikbakht F, Naderi N, Bakhshesh M, Azizi Y (2019) Apigenin attenuates doxorubicin induced cardiotoxicity via reducing oxidative stress and apoptosis in male rats. Life Sci 232:116623

70. Salehi B, Venditti A, Sharifi-Rad M, Kręgiel D, Sharifi-Rad J, Durazzo A, Lucarini M, Santini A et al (2019) The therapeutic potential of apigenin. Int J Mol Sci 20(6):1305